

UNDERSTANDING FRACTURE ORIENTATION BY REMOVING POLARIZATION DISTORTION FOR DIRECT SHEAR WAVES

Terence Campbell

*Department of Geological Sciences
The University of Texas at Austin*

Abstract

The progressive growth of onshore shale production (gas and liquids) to replace the increasing number of aging oil fields may necessitate the use of seismic shear wave data for full characterization of shale reservoir properties for defining and developing these resources, this includes descriptions of anisotropy for characterization of fractures (HTI) as well as the internal nature of the shales (VTI). The objective of this study is to document the distortion in polarization of seismic shear waves upon reflection, and address a correction, based on an understanding of shear amplitude versus incidence angle behavior, which corrects for the distortion at mid and far offset angles. This includes demonstration of the efficacy of the proposed correction by applying it to real shear wave source data. This should result in a minimized distorted amplitude response that arises from polarization distortion upon reflection. The apparent consistency of the null value (zero crossing) of the SV-SV reflectivity near 20-24 degrees for common density and velocity contrasts as well as the remarkably regular behavior of the SV-SV reflectivity curve following an $A+B\sin^2\Theta$ relation, may offer the opportunity for a stable correction with minimal sensitivity to detailed knowledge of contrasts in velocity & density. Some key questions must be addressed in gaining an understanding of shear wave distortion upon reflection for varying model data: 1) how do we address reflected polarization distortion for isotropic medium for varying incidence angles? 2) How do we apply this correction for isotropic medium and HTI medium which can be used to simulate real data? 3) Applications to real data and how distorted amplitudes can be corrected to identify real HTI anisotropy not observed in polarization distortion reflections.

INTRODUCTION

The goal of this study is to experimentally confirm and document the theoretically predicted distortion of polarization in seismic shear-wave reflections in both isotropic and anisotropic material and to evolve strategies to correct for this distortion. Thus, the basic hypothesis of this study is: a) Seismic shear waves undergo significant distortion in polarization upon reflection at non-normal angles of incidence and b) This distortion can be corrected with sufficient precision to allow interpretation of polarization information to infer bulk properties of the medium of wave propagation. This will require a full understanding of the factors that influence reflection of direct shear wave data and the role they play in characterization and evaluation of subsurface

Corrections for Polarization Distortion

reservoirs using S wave data, particularly polarization information. This investigation explores issues of variations and characterization of this distortion in polarization, what are some of its characteristics in both isotropic and anisotropic media and how effectively we can correct for this polarization distortion.

Interpretations of seismic shear waves including their variations in polarization are particularly useful in investigating the anisotropy of elastic media they propagate through and are reflected from. For such polarization information to be meaningful, however, there can be no distortion of polarization in the reflection process itself. Unfortunately, reflected shear waves do exhibit significantly modified polarizations associated solely with the reflection process, even in isotropic media. Typically, shear wave polarization is described in terms of orthogonal SV and SH coordinates defined by the source and receiver positions where the reflectivity is calculated for each orthogonal component (Figure 1). In analyzing shear wave reflectivity, an arbitrary polarization of the incoming shear wave is typically defined in terms of two the trigonometrically isolated orthogonal components SV & SH. For non-normal angles of incidence, the reflectivity of the individual SV & SH components can be quite different, leading to the change in the reflected polarization of the reflected wave (Figure 2) relative to the polarization of the incident wave. This distortion occurs even in the purely isotropic media. A corresponding example of this distortion exists in optics, where Brewster's (polarizing) angle has no reflectivity in the equivalent SV component, and all the reflected energy has solely SH polarization—totally independent of the incoming polarization.

Interestingly, analysis of the reflection phenomena of incident SV waves also shows SV reflectivity vanishes at a small range ($\sim 20^\circ - 25^\circ$) of incidence angles (Krohn, 1988; Gumble 2006; Lyons 2006). The apparent stability of this angle nearly independent of the contrast in the shear-wave impedance suggests that a correction for this effect may have only a weak dependence on our full knowledge of the actual values of velocities and densities across the reflecting interface. Thus, corrections may be possible with only modest sensitivity from our knowledge of the velocities and densities.

Simmons (2004) did identify the presence of what he has described as “cross-term” energy (even in isotropic media) when simulating or recording a 3D survey utilizing shear-wave sources and receivers. This results from variations in SV-SV and SH-SH energy being projected onto the receiver components with arbitrary 3D acquisition geometry and differences in SV and SH reflectivity. Our investigation expands on that work exploring issues with polarization analysis, and how to record the actual polarization information. A correction for the polarization distortions is in contrast to processing in pure SV & SH components, which preserve AVO interpretation by abandoning the polarization information. The polarization correction will be independent of (and actually at the expense of) the AVO information.

Corrections for Polarization Distortion

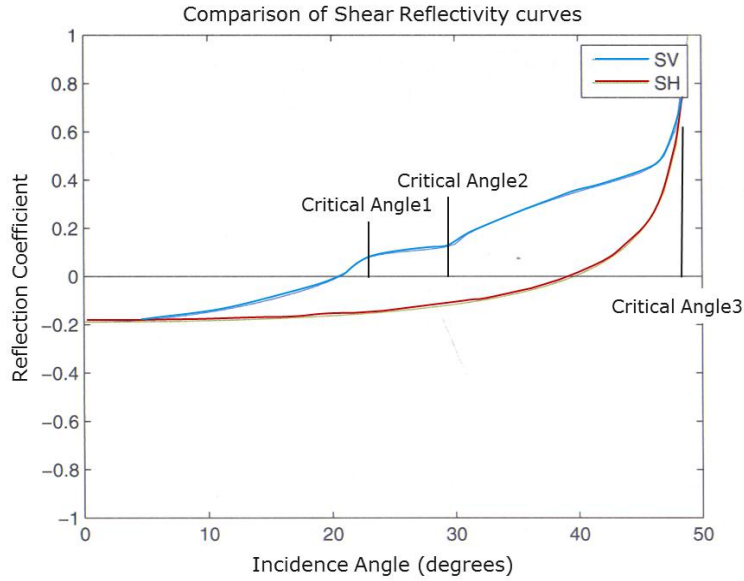


Figure 1. Reflection coefficient for SV-SV and SH-SH wave showing that the reflection coefficients vanish for some angle of incidence. Velocities and Density information for all the examples shown is given in table 1. The positions of the three critical angles associated with the incident SV wave are shown. The three critical angles relate to the P-wave mode converted and refraction into the lower layer (22°), the refracted mode converted P-wave in the upper medium (30°) and the refracted S-wave in the lower layer (49°). Note the single critical angle for the incident SH wave is at 49° the same as for the SV-SV refraction. The zero crossing is at 20° for SV and 39° for SH

| | P-velocity (km/sec) | S-velocity (km/sec) | Density (g/cc) |
|---------|---------------------|---------------------|----------------|
| Layer 1 | 3.0 | 1.5 | 2.0 |
| Layer 2 | 4.0 | 2.0 | 2.2 |

Table 1. Two layer isotropic model with carrying elastic properties

Corrections for Polarization Distortion

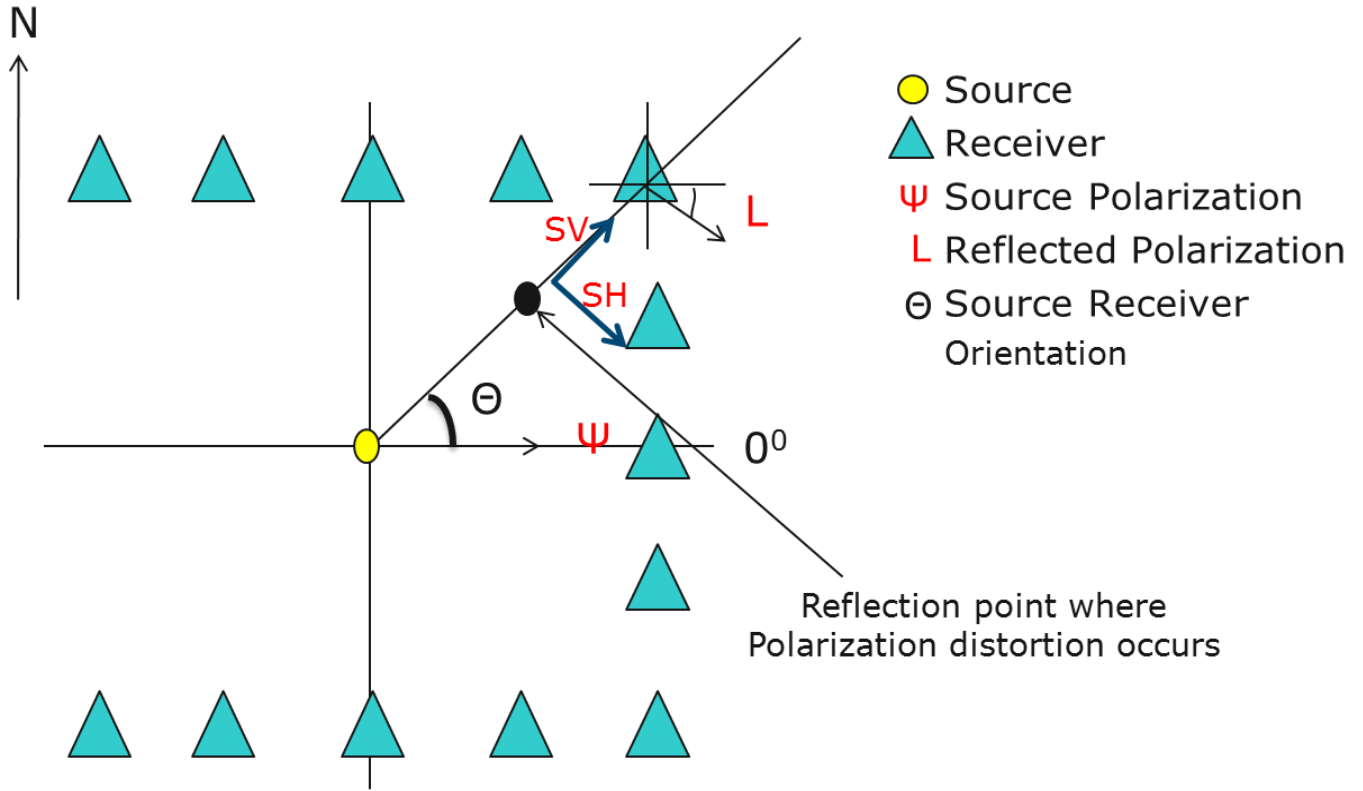


Figure 2. The geometric configuration of a 3D direct shear survey with a source polarization of 0° , and the associated terminology, where L is the polarization of the reflected wave is calculated in equations 8 and 9 and is quite different than the source polarization (from Lyons 2006).

SEISMIC P AND S WAVES

Seismic P waves and S waves are two types of seismic body waves propagate through solid materials (Sheriff and Geldart, 1995, p. 45, see figure 3). Primary (P) waves (equation 1) also known as compressional waves that respond to elastic properties and density of the material of that the waves propagate through. For P-waves this polarization (particle motion) is parallel to direction of wave travels (Tatham and McCormack, 1991). Shear waves (equation 2) however, respond to different combinations of elastic properties (shear modulus), density and are polarized in directions normal to the propagation direction.

$$P \text{ (primary) wave Velocity} = \sqrt{\frac{k+4/3\mu}{\rho}} \quad (1)$$

$$S \text{ (Shear) wave Velocity} = \sqrt{\frac{\mu}{\rho}} \quad (2)$$

K = Bulk modulus

μ = shear modulus

ρ = Density

Corrections for Polarization Distortion

Their polarization (particle motion) is normal to the direction of wave travel and thus may be in any direction normal to the propagating ray direction (Tatham and McCormack, 1991). Shear waves however, are commonly resolved into S_T and S_R , orthogonal, transverse and radial components corresponding to SH & SV respectively (figure 4). Ultimately the shear waves propagating through an anisotropic medium will be naturally polarized in the natural axes of anisotropy of the medium (Gumble, 2006). That is fast shear component (S1) will be polarized in the direction of the higher velocity of the medium, whereas the slower shear component (S2) will be polarized orthogonal to S1 (figure 5). Significantly the ray paths of the two components are essentially identical. The normalized time delay between the S1 and S2 components may be related to the magnitude of the anisotropy of the medium (Tatham et al. 1992). This effect is identified to the birefringence of optical waves used in optical mineralogy.

FIELD DATA ACQUISITION

For 2D acquisition along a profile, the polarizations of the direct shear-wave sources and receivers are generally oriented horizontally in-line (parallel to) and cross-line (normal to) the shot, or profile, direction. Thus, the source polarizations are always in the vertical plane, or normal to the plane, defined by the location for any source and receiver pair along the line (see figure 4). For 3D acquisition, the sources and receivers are located on an aerial surface and the individual source and receiver positions may be described in terms of x-y Cartesian coordinates, where x commonly corresponds to east and north corresponds to y. These x-y coordinates may be considered ‘field’ coordinates—controlled entirely by the survey design and totally independent of any subsurface geologic properties. Further, the actual polarizations of the direct shear sources and receivers are commonly oriented in the x and y direction. Thus, the azimuthal direction connecting a pair of source and receiver positions will not, in general, be oriented in either the x or y direction. This leads to each source and receiver orientation not generally aligned with the vertical plane connecting the source and receiver position. To consider the result of the reflection between an arbitrary source and receiver pair, each x and y source component must be trigonometrically projected into SV and SH components relative to the source-receiver azimuth for the individual source-receiver pair and reflection coefficients calculated for each independent component. The individual x and y components of each source is then recorded by the x and y components of each receiver. Each of these receiver components can be combined to define the actual polarization of the reflected wave. A basic thesis of this study is that, the actual polarization of the recorded shear-wave reflection will not, in general, be the same as the source actual polarization—even in purely isotropic materials.

Historically, based on two dimensional profile recording, the complexity of all these components has not become an issue until 3D seismic acquisition became common. Prior to 3D acquisition, data were generally recorded along a single line with the acquisition orientation set-up in an SV and SR configuration. Three-dimensional recording has led to additional complexities in the geometry and associated complexities in the meaning of the polarizations of the reflections.

The radial component contains predominantly SV waves and P-waves (see fig. 2), while the cross-line transverse-source, transverse-receiver component contains only SH waves in an

Corrections for Polarization Distortion

isotropic flat-layered earth. SH data are simplified in that SH waves reflect and transmit only to SH, unlike SV propagation, which is coupled with P.

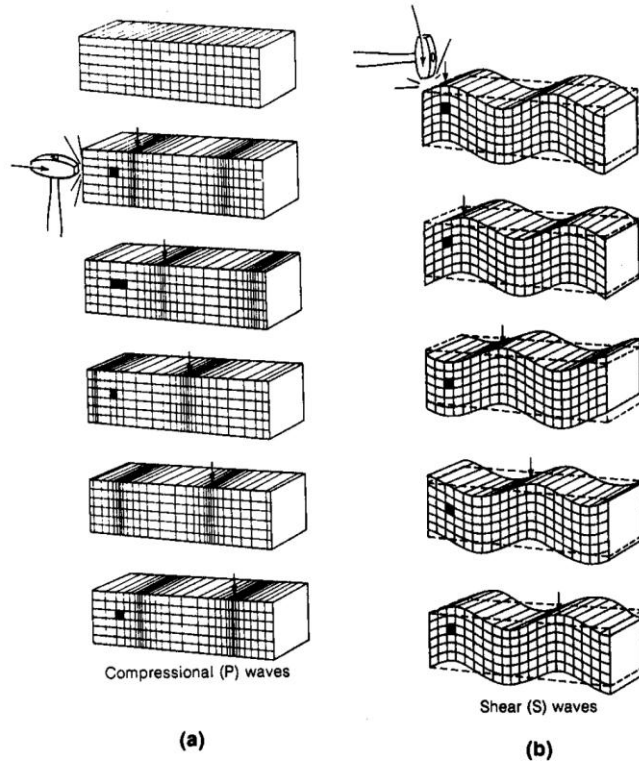


Figure 3. Particle motion during passage of plane body waves, (a) P-waves and (b) S-waves (Sheriff and Geldart, 1995, p.45)

POLARIZATION INFORMATION

As discussed in the introduction polarization information to be meaningful in interpretation of the properties of the media it is propagating through there must be no distortion of polarization in the reflection process itself. Reflected shear waves, however do exhibit significantly modified polarizations associated solely with the reflection process. Analysis of shear wave reflectivity, a general polarization of the incoming shear wave is typically defined in terms of two trigonometrically separated orthogonal components (SV & SH) related to the source and receiver locations on the surface. For non-normal angles of incidence, the reflectivity of the individual SV & SH components can be quite different leading to the change upon reflection in the reflected polarization of the incoming wave. This is true even in the purely isotropic media.

Corrections for Polarization Distortion

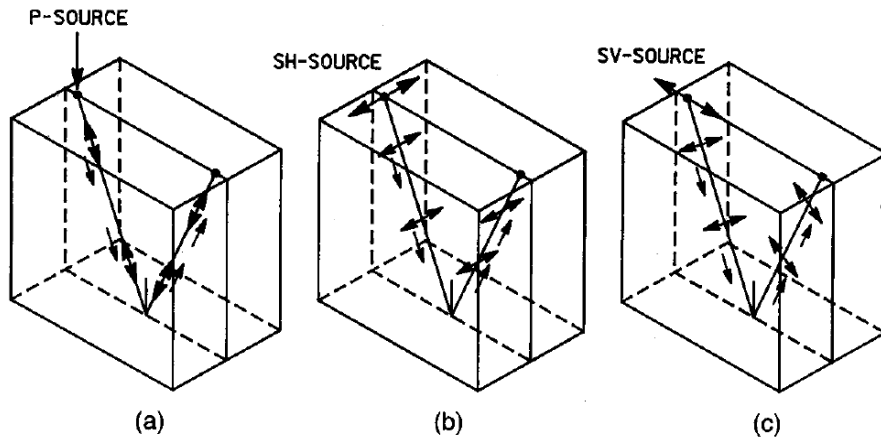


Figure 4. Ray propagation and polarization directions, with propagation shown by smaller arrows next to rays, and particle motion shown by two-headed arrows for (a) P-P, (b) SH-SH and (c) SV-SV waves (Tatham and McCormack, 1991, p.14).

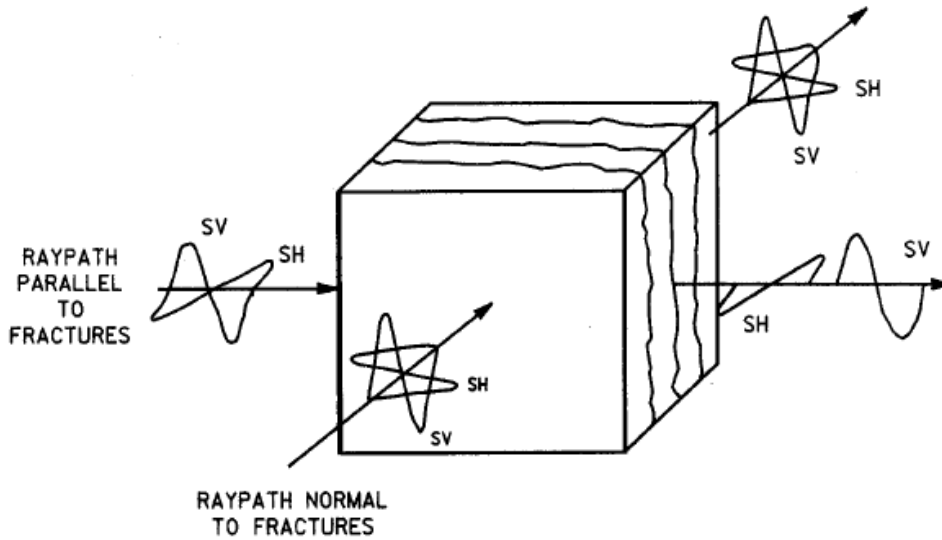


Figure 5. The effect of the vertical fractures on S-wave propagation. Note the relationship between fracture orientation and polarization of S-waves exiting the medium (Tatham and McCormack, 1991, p.77).

CALCULATION OF POLARIZATION DISTORTION

Firstly we note that all the seismic shear sources considered are from direct (horizontal) shear wave sources with specific horizontal polarities. The input source polarizations are projected into SV and SH components for each specific source-receiver azimuth. To simulate the reflection process, reflection coefficient are calculated and are then applied to the individual incoming SV and SH components. The individual SV and SH reflection components are then combined to produce the resultant polarization of the reflected shear wave. Figures 6 and 7 show the resultant reflection polarizations for separate X and Y oriented shear sources respectively into an areal surface array of X and Y oriented receivers. The results plotted as the actual vector polarizations of the shear wave reflectors. Note the wide variation of the resultant reflection polarization shear-to-shear reflection for a single source polarization, even for this purely isotropic media. Again, this distortion results from the input source not being initially aligned with the source-receiver azimuth (typical for a 3D surface survey) and the dramatic differences in the SV and SH components of the actual reflectivity. The offset associated with the SV zero crossings is also shown. Note that at this offset (analogous to the Brewster's polarization angle of optics), only an SH polarization is observed.

SIMPLIFICATION OF THE SV AND SH REFLECTIVITY RELATIONS

To develop a simple and useful correction for this distortion, we further simplify the Zoeppritz equations by using approximations of Spratt (1993) and Lyons (2006).

Spratt (1993) proposed, using typical small angle and contrast in velocity and density assumptions, the following forms for the reflectivity relationships.

$$R_{SV-SV} = A + B_{SV} \sin^2 j \quad (3)$$

and

$$R_{SH-SH} = A + B_{SH} \sin^2 j \quad (4)$$

Lyons (2006), based on some of the simplifying assumptions, modified the SH reflectivity to:

$$R_{SH-SH} = A + B_{SH} \tan^2 j \quad (5)$$

Since both the SV-SV and SH-SH reflectivity curves do have zero crossings for reasonable angles on incidences (about 20° for SV and 40° for SH waves), we can 'fit' the form of anticipated reflection curves quite well to any Zoeppritz curve from the observed reflectivity value at zero offset and knowledge of the zero-crossing. From this, we can estimate A and B by setting reflectivity to zero at the assumed zero crossing. These approximations are shown in Figures 8 and 9 for the zero crossing values of 22° and 40° from Figure 2. It is worth noting that, for the SV curve, the zero crossing has a rather narrow range of angles, near 20°, for a wide range of interface contrasts. Overall, the SH curve tends to be rather simple. These two observations suggest that the use of such a simple form for the reflectivity curves may be readily justified, and lead to only a modest sensitivity to errors in the estimation of the zero crossings using to estimate B_{SV} and B_{SH} .

Corrections for Polarization Distortion

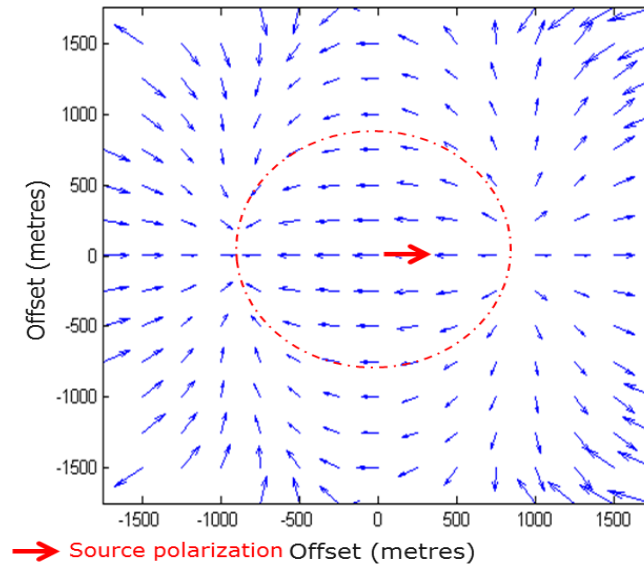


Figure 6. Observed simulated polarizations in a single 3D source record (source at center) of a 3D survey of isotropic media (map view) corresponding to a reflector depth of 2000m. The length of the vectors indicates the amplitude of the recorded data, and the orientation of the vectors indicates the observed polarization. The circle indicates the offset associated with the zero crossing (null value) ($j=22^0$) of the SV reflectivity (source is polarized due east).

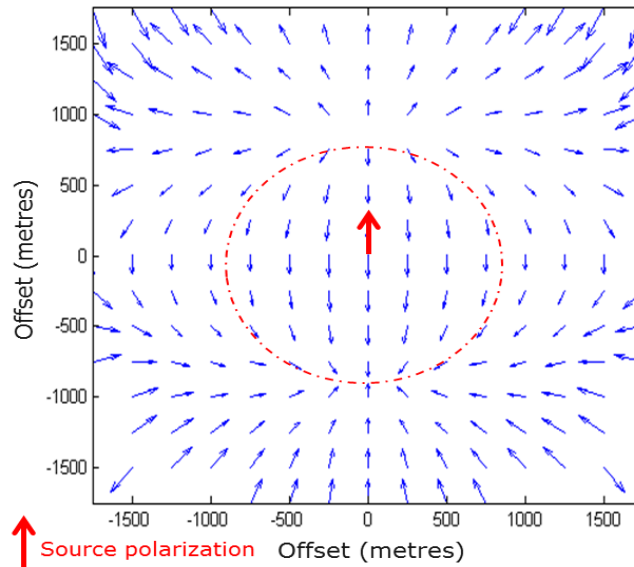


Figure 7. Observed simulated polarizations in a single source record 3D survey of isotropic media (map view) corresponding to a reflector depth of 2000m. The length of the vectors indicates the amplitude of the recorded data, and the orientation of the vectors indicates the observed polarization. The circle indicates the offset associated with the zero crossing (null value) ($j=22^0$) of the SV reflectivity (source is polarized due north)

Corrections for Polarization Distortion

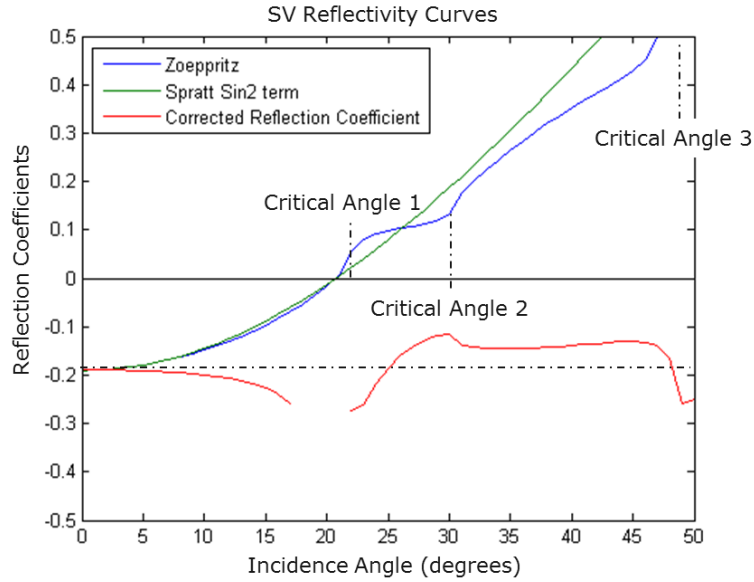


Figure 8. Comparing the full Zoeppritz equations to a two term Sin^2 approximation, describing SV reflections. The model parameters are listed in Table 1. There is excellent agreement between the two through an incident angle of about 30° . The small departure at $j=22^\circ$ corresponds to the critical angle for the first refracted P-wave. There are also two additional critical angles at 30° & 49° corresponding to the internal refraction in the upper layer and the shear wave refraction in the lower layer. The suggested corrections are also applied to the actual Zoeppritz curve. The unstable region near the zero crossing is omitted.

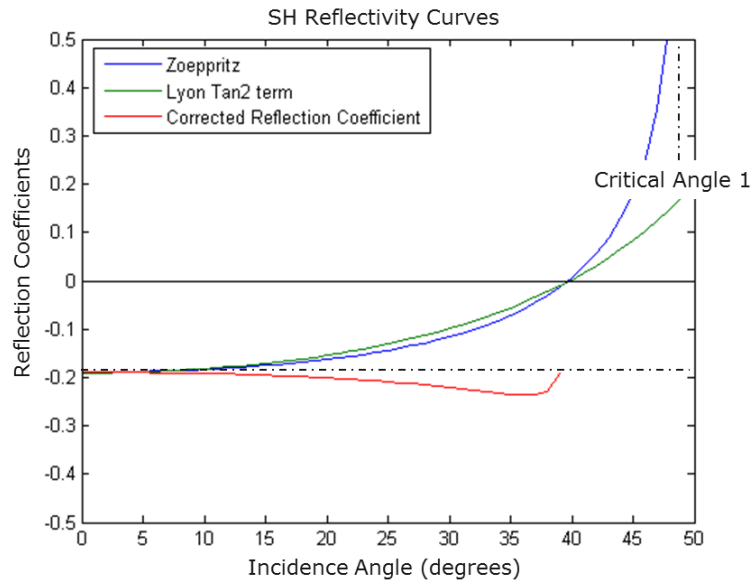


Figure 9. Comparing the full Zoeppritz equations to a two term \tan approximation, describing SH motion. The model parameters are listed in Table 1. There is good agreement between the two through an incident angle of 40° . The suggested corrections are also applied to the actual Zoeppritz curve. The correction is omitted near the zero crossing.

Corrections for Polarization Distortion

CALCULATION OF A POLARIZATION CORRECTION

A corrected reflection coefficient can be used to minimize the amplitude change caused by the distortion upon reflection of the S-wave from a direct S wave source. The required B_{SV} and B_{SH} values can be calculated by assuming that $A=1$ and $R=0$ for the zero crossing values of $jz=20^0$ and 40^0 for SV and SH respectively (obtained from figure 8 & 9).

Thus:
$$0 = 1 + B_{SV} \sin^2 jz \quad (6)$$

and

$$0 = 1 + B_{SH} \tan^2 jz \quad (7)$$

So

$$B_{SV} = -1/\sin^2 jz \quad (8)$$

and

$$B_{SH} = -1/\tan^2 jz \quad (9)$$

The correction is minimized by the following equations:

$$R_{SV-SVCOR} = R_{SV-SV} * (1/ (1+B_{SV} \sin^2 j)) \quad (10)$$

$$R_{SH-SHCOR} = R_{SH-SH} * (1/ (1+B_{SH} \tan^2 j)) \quad (11)$$

These corrections $R_{SV-SVCOR}$ and $R_{SH-SHCOR}$ are shown in figures 8 and 9. There is an unstable region near jz , so no meaningful correction can be applied in that area.

PRELIMINARY RESULTS

To show corrected distorted polarization we compare the original polarization plots with the corrected polarization plots using a simple trigonometric relationship for polarization distortion calculated from figure 2.

$$L = \tan^{-1} \left[\frac{\cos(\theta - \psi) R_{SV-SV}}{\sin(\theta - \psi) R_{SH-SH}} \right] + \theta - 90 \quad (12)$$

$$L = \tan^{-1} \left[\frac{\cos(\theta - \psi) R_{SV-SV}}{\sin(\theta - \psi) R_{SH-SH}} \right] + \theta + 90 \quad (13)$$

Now we apply the corrected distorted polarization equations to figures 6 & 7 and obtain corrected values for polarization distortion (figure 10 & 11). Note the consistency of the polarization out to rather large effects, approaching 50% of reflector depth.

Corrections for Polarization Distortion

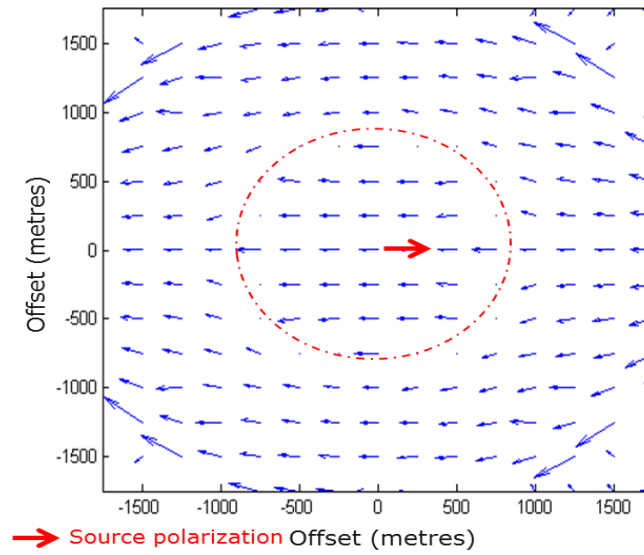


Figure 10. Polarization corrections applied to the simulated polarization distortions in a 3D record of isotropic media (map view) corresponding to a reflector depth of 2000m. The length of the vectors indicate the amplitude of the data, and the orientation of the vectors indicates the observed polarization (source is polarized due east). The corrections used a zero crossing of 20° SV and 40° SH from figures 4 & 5 for actual velocities used in the modeling.

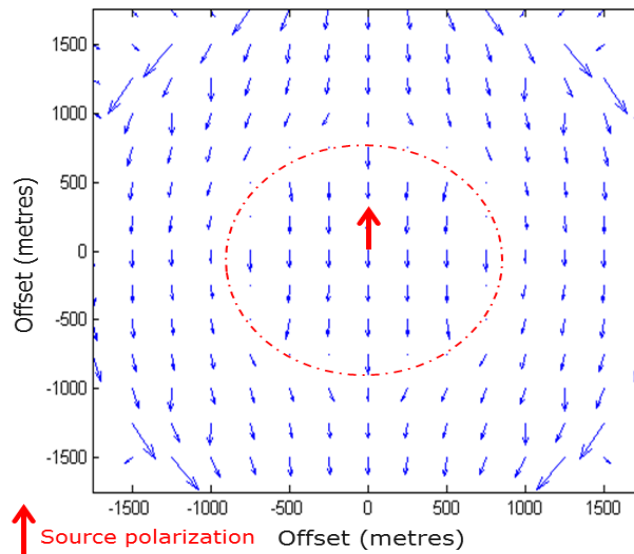


Figure 11. Polarization corrections applied to the simulated polarizations in a 3D survey of isotropic media (map view) corresponding to a reflector depth of 2000m. The length of the vectors indicate the amplitude of the corrected data, and the orientation of the vectors indicates the corrected polarization (source is polarized due north). The corrections used a zero crossing of 20° SV and 40° SH from figures 4 & 5 for actual velocities used in the modeling.

SENSITIVITY ANALYSIS

Sensitivity analysis for the apparent unchanging value of the SV-SV reflection zero-crossing is performed to understand what parameters affect the value of the SV-SV zero crossing that distorts reflection data for both SV and SH waves, reflections. Figures 12 and 13 shows preliminary models for varying values of shear velocity. The R_{SV-SV} reflectivity is quite predictable, especially the zero-crossing in the reflectivity curve being at a nearly constant position for a wide range of contrasts in V_P , V_S and ρ . We can hypothesize a stable correction for polarity change for a wide range of contrasts in sedimentary rocks. The question comes as to how stable this correction really is, and what happens when we introduce anisotropic material especially HTI symmetry. Effects and corrections for distortion in polarization for various model data will be explained to address analogues for the proposed data set. The synthetic models are generated using internally simulation modeling software, which uses contour integration in the complex frequency-wavenumber domain to compute seismograms and thus produce correct, interpretable amplitudes (Mallick and Frazer, 1987). When the synthetic models are understood then we will apply the correction to a real data set.

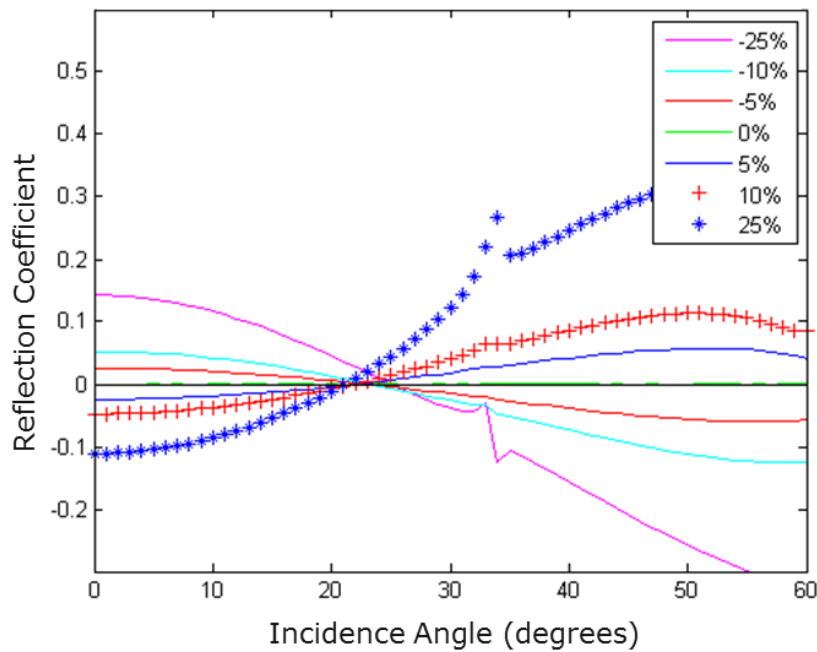


Figure 12. RSV-SV reflection coefficient with changes in shear wave velocity contrast. Initial $V_P/V_S = 1.8$, density = 2.2g/cc; density and V_P is held constant for both media contrast and the shear wave velocity contrast varies +/- 25%. Note the effect of critical angles at large contrasts in V_S . Also note the consistency of the zero-crossing near 24° .

Corrections for Polarization Distortion

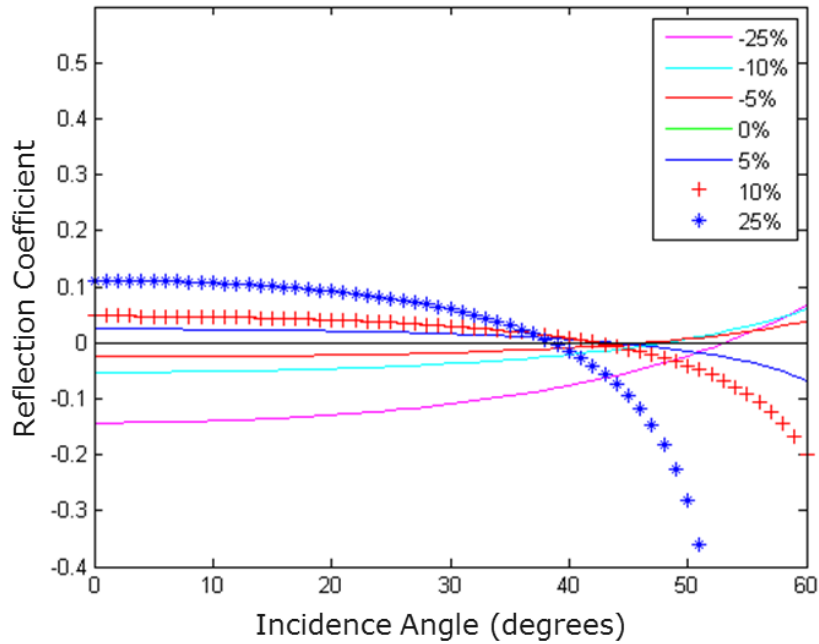


Figure 13. RSH-SH reflection coefficient with changes in shear wave velocity contrast. Initial $V_P/V_S = 1.8$, density = 2.2g/cc; density and V_P is held constant for both material contrast and the shear wave velocity contrast varies +/- 25%. The curves are quite similar in character and only these constants approaching 25% deviate from a constant angle.

COMPLICATIONS TO POLARIZATION DISTORTION

Anisotropy is a variation in some observed parameter with direction. In the case of seismic shear waves, this direction can be either propagation direction or polarization direction. Stated differently seismic anisotropy is the phenomenon of a medium exhibiting faster seismic velocity in one direction than in another direction, or in the case of shear waves, differences in seismic velocity in the same direction if the shear-waves have different polarizations. An excellent review of anisotropy and how it relates to lithological and reservoir parameters are available in Thomsen (2002). Since S-waves are transversely polarized, they can be especially useful for characterizing anisotropic parameters. This results from their sensitivity to polarization direction even for a single ray propagation direction. Any arbitrary polarization of an S-wave will ultimately be polarized in the natural axes of anisotropy of the medium. The fast shear (S1) will be polarized in the direction of the higher velocity of the medium, whereas the slower shear component (S2) will be polarized orthogonal to S1 (figure 14).

Significantly, the ray paths of the S1 and S2 components are identical for the symmetry and ray-paths assumed. The normalized time delay between the S1 and S2 components may be considered a measure of the magnitude of the anisotropy of the medium. Anisotropy associated with geologic formations may be the result of a preferential fracture orientation. Fracture orientation may be an important factor in reservoirs, dictating the flow of hydrocarbon during production, hence the practical usefulness of anisotropy analysis. There are many models of

Corrections for Polarization Distortion

anisotropy that can be used to simplify the analysis; typically transversely isotropic media with different axes of symmetry (VTI and HTI respectfully, Tatham and McCormack, 1991). Vertical fracture sets in the earth are a source of anisotropy in seismic velocity (Crampin, 1983) and there may be characterized as transversely isotropic media with a horizontal axis of symmetry (HTI) (figure 15). Sources of VTI seismic anisotropy include horizontal bedding and lithology (alignment of clay minerals in shale (Tatham and McCormack, 1991, figure 15). These characterizations may prove useful in characterizing resource shales. Complications can arise from the presence orthorhombic symmetries arising from intersecting fracture sets or intersecting fracture sets with horizontal bedding.

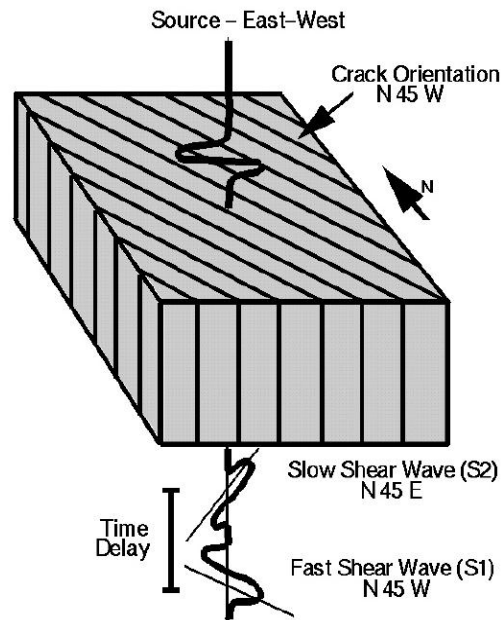


Figure 14. Model of shear wave splitting, or birefringence. An arbitrarily polarized shear wave enters the fractured medium from above. In this case, the input shear-wave is polarized east-west within the medium the one component of the shear wave is polarized in the direction of the fractures and becomes S1, or the fast shear wave. The remaining component is polarized in the direction perpendicular to the fracture orientation and becomes the slow shear wave, or S2. (This example is diagrammatic of the general case, but also corresponds to evidence relating to shear-wave birefringence in the Weyburn oil field found in sonic logs (modified from Bowman et al., 1987 and Martin and Davis, 1987).

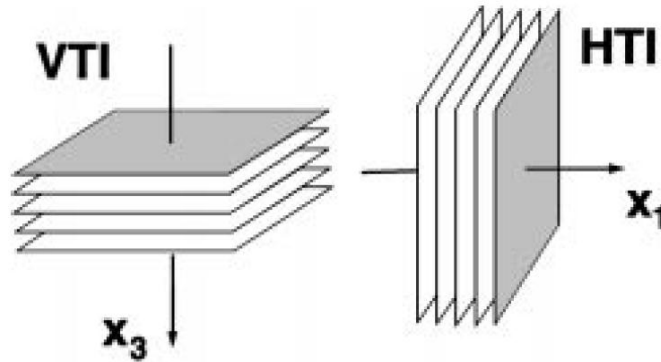


Figure 15. Sketch of VTI and HTI models. Reflections of P-waves confined to the two vertical symmetry planes, here called the symmetry-axis plane and the azimuthally isotropic plane. Shear waves polarized parallel and normal to the isotropy plane have different vertical velocities (Ruger, 1996).

POLARIZATION DISTORTION IN TRANSVERSELY ISOTROPIC MEDIUM

We will consider a fractured medium described as HTI, transverse isotropy with a horizontal axis of symmetry (figure 16). Due to the complexity of anisotropy polarization analysis for HTI medium would result in inaccurate conclusions, if the anisotropy is not taken into account. Since we are dealing with SV and SH polarizations, shear wave AVO azimuthal analysis will be considered in the symmetry and isotropy plane. The waves whose source-receiver geometry is parallel to the isotropy plane are in the strike direction (parallel to fractures), while the waves whose source-receiver direction is parallel to the symmetry plane (normal to fracture direction) are in the symmetry direction. The fast shear waves S1 is polarized within the isotropy plane and the slow S-wave, S2 is polarized in the symmetry plane. Figure 17 defines the polarization and propagation directions for shear waves (Ruger, 1996). Table 2 shows the anisotropic parameters used to model the isotropic over HTI medium where we predict changes from the standard isotropic plots.

MODELING HTI PARAMETERS

We repeat the process for simulating a 3D survey and expand the experiment to model an isotropic medium over an anisotropic medium (figure 18). Direct shear data is simulated in a three dimensional model of an isotropic medium over an anisotropic medium using a Fourier frequency-wave number numerical modeling method (Mallick and Frazer, 1987). The parameters used to create the isotropic over anisotropic model are outlined in Table 2. For the second part of the study, polarization analysis, the model included: 1) Direct S-wave with an isotropic medium overlying an anisotropic half-space. Thomsen parameters (Thomsen, 1986) are summarized in table 2 for the anisotropic layer and the acquisition geometry is described in Figure 18. The fractured models include HTI (horizontal transverse isotropy) symmetry. The orientation of the anisotropy (transverse isotropy with a horizontal axis of symmetry, HTI) is oriented east in the map view. The simulated field data is kept constant while the anisotropic medium is rotated 360^0 , so that the receivers will be in radial (SV) and transverse (SH)

Corrections for Polarization Distortion

orientations. The amplitude correction is applied and the corrected polarizations are calculated in a method similar to the method used for the earlier models, but modified to be used in all four quadrants of the source-receiver azimuth. The results for a source orientation in the east direction (0° orientation) are shown in Figure 19 (fractures oriented due east) and Figure 21 (fractures oriented 30° north of east, and the results for the polarization corrections are shown in Figure 20 and Figure 22 respectively.

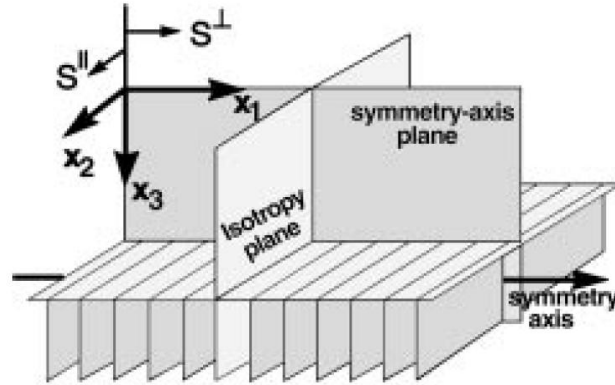


Figure 16. Sketch of an HTI model. Reflections of P-waves confined to the two vertical symmetry planes, here called the symmetry-axis plane and the isotropy plane, are discussed in the text. Shear waves polarized parallel and normal to the isotropy plane have different vertical velocities (Ruger, 1996).

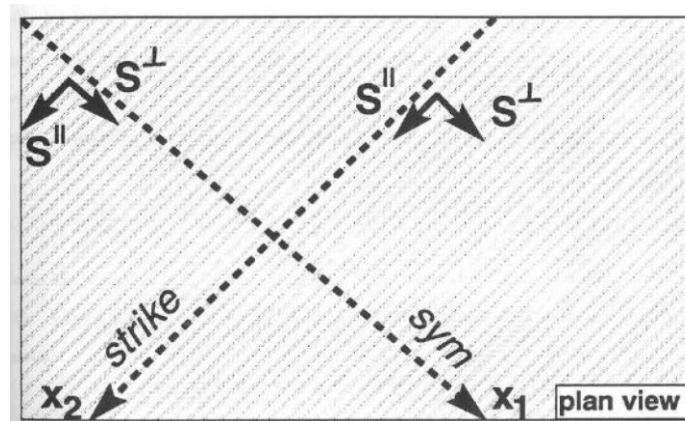


Figure 17. Plan view of HTI medium, with the source and receiver acquisition directions, strike and symmetry directions with the polarization direction for the fast and slow shear waves ($S^\perp=S2$; $S^\parallel=S1$). Amplitude with offset analysis will be performed in the strike and symmetry directions which represent the isotropy and the symmetry-axis planes, respectively (Ruger, 1996).

Corrections for Polarization Distortion

| | Model |
|------------------------------|--|
| Layer1 (Isotropic) | $V_p=3.0\text{km/sec}$ $V_s=1.5\text{km/sec}$ $\rho=2.00\text{g/cc}$ |
| Layer 2 (HTI anisotropic) | $V_p(0)=4.0\text{km/sec}$ $V_s(0)=2.0\text{km/sec}$ $\epsilon=0.30$ $\delta=0.10$ $\gamma=0.05$ Fracture Strike=East $\rho=2.2\text{g/cc}$ |

Table 2. Properties of an anisotropic synthetic media, where V_p is the compressional wave velocity, V_s is the shear wave velocity. $V_p(0)$ and $V_s(0)$ are the vertical P-wave and S-wave velocities in the anisotropic media, respectively. $\epsilon(v)$, $\delta(v)$, and $\gamma(v)$ are the exact Thomsen parameters of the equivalent VTI media.

Note that there are small changes in the length of the arrows actually coinciding with the input polarization, consistent with the anisotropic character of the lower layer. After applying several simulations to different synthetic models for gamma values greater than 2% it appears to make no difference which way the source is oriented, the observed and corrected polarizations are all correctly oriented in the direction of the lower layer's anisotropy. For large values of anisotropy (greater than 10%) it appears that uncorrected data properly defines the orientation of the anisotropy – so no correction would be required with these high levels. However for the low anisotropy of 1%, the observed and corrected polarizations have no real differences from the simple isotropic over isotropic case because shear wave splitting seems to not occur.

Table 3 below outlines various models where we applied Ruger's equations to calculate the reflection coefficients for an HTI medium (Ruger, 2001). I was able to calculate the zero crossing values which are outlined in Figures 23 and 24 for the various models and these values were used to correct for polarization distortion. Figure 23 and 24 plots also show the relative stability of the zero crossing values for a source parallel and for a source perpendicular to HTI axis symmetry in the varying models. Due to the consistency in the zero-crossing values it can be noted that a universal correction may be applied for sources parallel to strike direction and sources normal to strike direction for varying levels of anisotropy.

DISCUSSION

Anisotropy presents a particular challenge and opportunity in understanding the ever expanding shale gas plays. On land seismic data, some have approached the acquisition problem by restricting the data to very small offsets and have attempted to deal with the overwhelming ground roll interference by the use of source and receiver arrays and/or abundant trace mixing in data processing. Others have rotated horizontal components into S1 and S2 directions extracted from nearby VSP studies. Still others have worked entirely in SV and SH components.

Corrections for Polarization Distortion

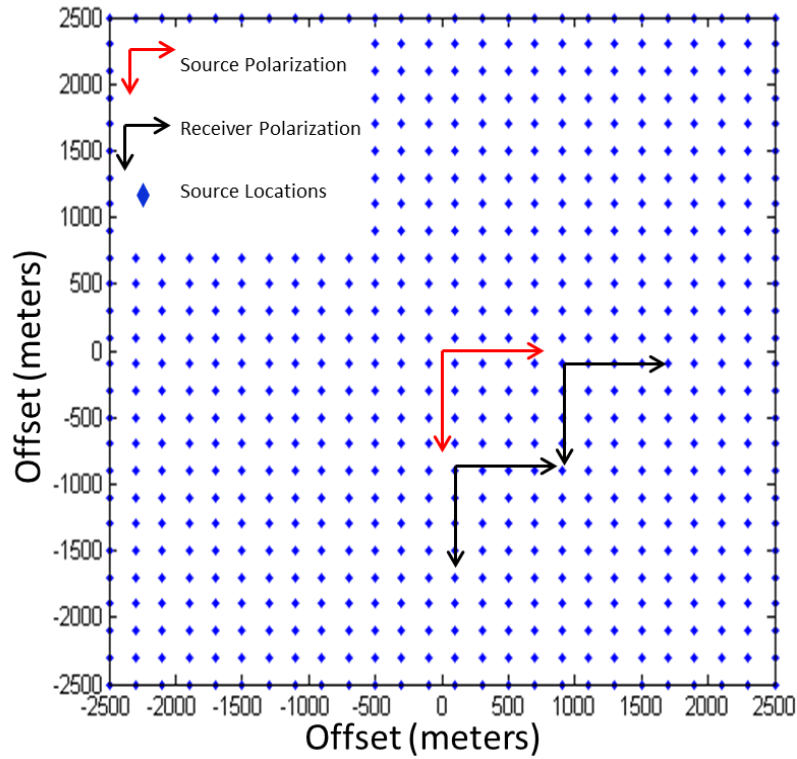


Figure 18. Acquisition geometry of the synthetic models. Receivers are positioned every 100m in both X and Y directions with the source located at (0, 0). The black arrows indicate receiver orientations and the red arrows indicate source orientations depending on the source directions.

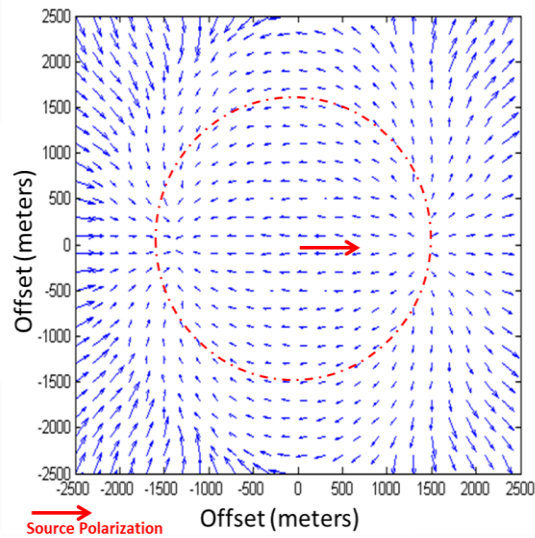


Figure 19. Observed simulated polarizations in a single 3D source record (source at center) of a 3D survey (map view) corresponding to a reflector depth of 2000m. The circle indicated the offset

Corrections for Polarization Distortion

corresponding to an incidence angle of 22° (the SV-SV zero crossing). The length of the vectors indicate the amplitude of the recorded data, and the orientation of the vectors indicates the observed polarization (source is polarized due east). Note the fractures are oriented east – west. Thomsen parameters used are; $\Gamma = 0.05$, $\Delta = 0.10$, $\epsilon = 0.30$.

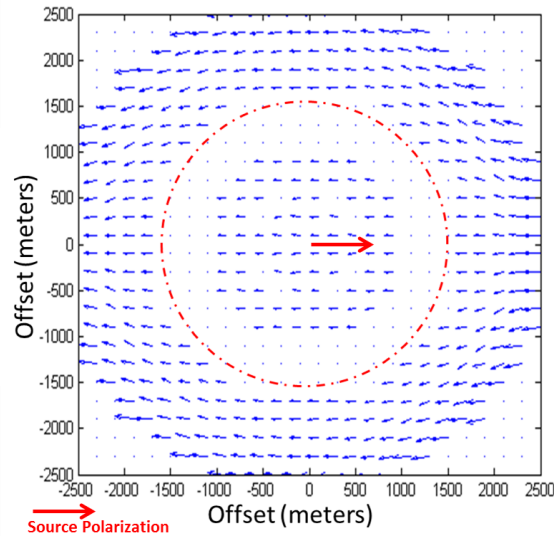


Figure 20. Polarization corrections applied to the simulated polarization distortions in a 3D record (map view) corresponding to a reflector depth of 2000m. The circle indicated the offset corresponding to an incidence angle of 22° (the SV-SV zero crossing). The length of the vectors indicate the amplitude of the data, and the orientation of the vectors indicates the observed polarization (source is polarized due east). The corrections used a zero crossing of 22° SV and 50° SH. Note the fractures are oriented east – west. Thomsen parameters used are; $\Gamma = 0.05$, $\Delta = 0.10$, $\epsilon = 0.30$.

Azimuthal anisotropy effects can then be recognized and analyzed by monitoring the reflection signal (in radial transverse coordinates) from the top and the base of the fractured reservoir interval as a function of offset and azimuth. Reflections from the base of a fractured interval may be more sensitive to the fractures than reflections from the top because the base reflections have traveled through the cracked interval. There are many important issues to be addressed in the effective utilization of 9-C-3-D data set, such as the Sycamore field Oklahoma and in particular multicomponent seismic data in general. At this point, removing polarization distortion from the reflection data is important in extracting fracture characterization hence rotation of the field coordinate data is essential in understanding azimuth variation for polarization distortion.

This polarization distortion is complicated because when we acquire shear wave seismic data *SH*, *SV*, and *P*-waves mix together in variable proportions which confuses attempts at processing and interpretation. Typically after acquiring land seismic data the processing involves the use of Alford rotation (Alford, 1986), for detecting the presence of azimuthal anisotropy produced by vertical cracks (Simmons, 2004). Using Alford rotation to in pre-processing of 3D seismic data

Corrections for Polarization Distortion

maybe the wrong approach because it's strictly valid only at normal incidence where there is no distinction between *SH* waves and *SV* waves.

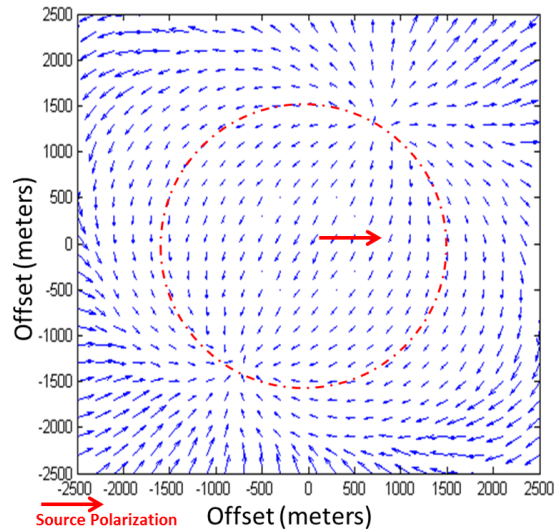


Figure 21. Observed simulated polarizations in a single 3D source record (source at center) of a 3D survey (map view) corresponding to a reflector depth of 2000m. The circle indicated the offset corresponding to an incidence angle of 22° (the SV-SV zero crossing). The length of the vectors indicate the amplitude of the recorded data, and the orientation of the vectors indicates the observed polarization (source is polarized due east). Note the fractures are oriented at an orientation of 30° degrees from north. Thomsen parameters used are; Gamma = 0.05, Delta=0.10, Epsilon=0.30.

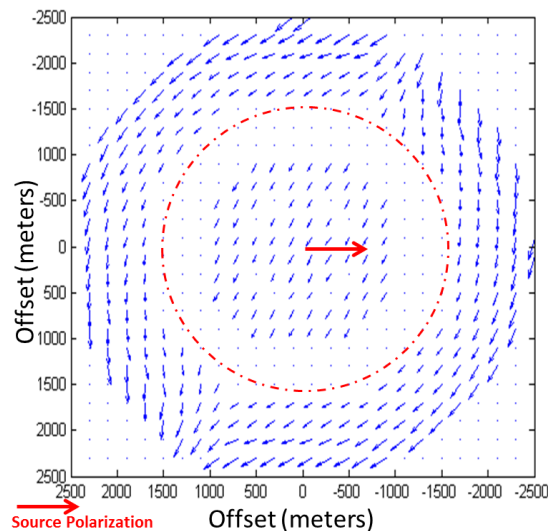


Figure 22. Observed simulated polarizations in a single 3D source record (source at center) of a 3D survey (map view) corresponding to a reflector depth of 2000m. The circle indicated the offset

Corrections for Polarization Distortion

corresponding to an incidence angle of 22° (the SV-SV zero crossing). The length of the vectors indicate the amplitude of the recorded data, and the orientation of the vectors indicates the observed polarization (source is polarized due east). The corrections used a zero crossing of 22° SV and 50° SH. Note the fractures are oriented at an orientation of 30° degrees from north. Thomsen parameters used are; $\Gamma = 0.05$, $\Delta = 0.10$, $\epsilon = 0.30$.

| | Model 1 | Model 2 | Model 3 | Model 4 |
|---------|--|--|--|--|
| Layer 1 | $V_P = 3.0 \text{ km/sec}$ $V_S = 1.5 \text{ km/sec}$ $\rho = 2.00 \text{ g/cc}$ | $V_P = 3.0 \text{ km/sec}$ $V_S = 1.5 \text{ km/sec}$ $\rho = 2.00 \text{ g/cc}$ | $V_P = 3.0 \text{ km/sec}$ $V_S = 1.5 \text{ km/sec}$ $\rho = 2.00 \text{ g/cc}$ | $V_P = 3.0 \text{ km/sec}$ $V_S = 1.5 \text{ km/sec}$ $\rho = 2.00 \text{ g/cc}$ |
| Layer 2 | $V_P(0) = 4.0 \text{ km/sec}$ $V_S(0) = 2.0 \text{ km/sec}$ $\epsilon = 0.30$ $\delta = 0.10$ $\gamma = 0.02$ $\rho = 2.2 \text{ g/cc}$ | $V_P(0) = 4.0 \text{ km/sec}$ $V_S(0) = 2.0 \text{ km/sec}$ $\epsilon = 0.30$ $\delta = 0.10$ $\gamma = 0.05$ $\rho = 2.2 \text{ g/cc}$ | $V_P(0) = 4.0 \text{ km/sec}$ $V_S(0) = 2.0 \text{ km/sec}$ $\epsilon = 0.30$ $\delta = 0.10$ $\gamma = 0.10$ $\rho = 2.2 \text{ g/cc}$ | $V_P(0) = 4.0 \text{ km/sec}$ $V_S(0) = 2.0 \text{ km/sec}$ $\epsilon = 0.01$ $\delta = 0.01$ $\gamma = 0.01$ $\rho = 2.2 \text{ g/cc}$ |

Table 3. Properties anisotropic synthetic media, where V_P is the compressional wave velocity, V_S is the shear wave velocity. $V_P(0)$ and $V_S(0)$ are the vertical P-wave and S-wave velocities in the anisotropic media, respectively. $\epsilon(v)$, $\delta(v)$, and $\gamma(v)$ are the exact Thomsen parameters of the equivalent VTI media.

Corrections for Polarization Distortion

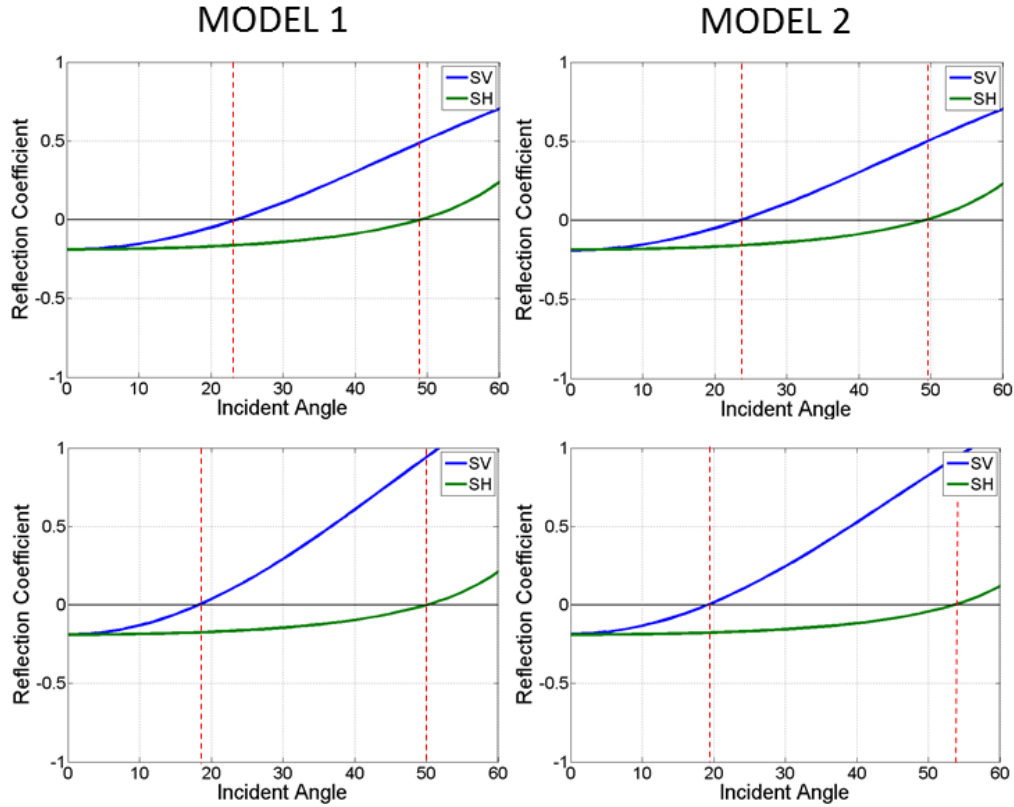


Figure 23. Shear-wave AVO. SH and SV reflection coefficients as a function of incidence angle. The interfaces are outlined above in table 3 and the graphs are calculated using Ruger’s equation for Isotropic over Transversely Isotropic medium. Note the red vertical lines show the zero crossings for the various models which are used to identify singularities in the polarization correction analysis. The top graph the source is oriented parallel to fractures and the lower plots the source is oriented perpendicular to fractures. Note there is no change in zero crossing.

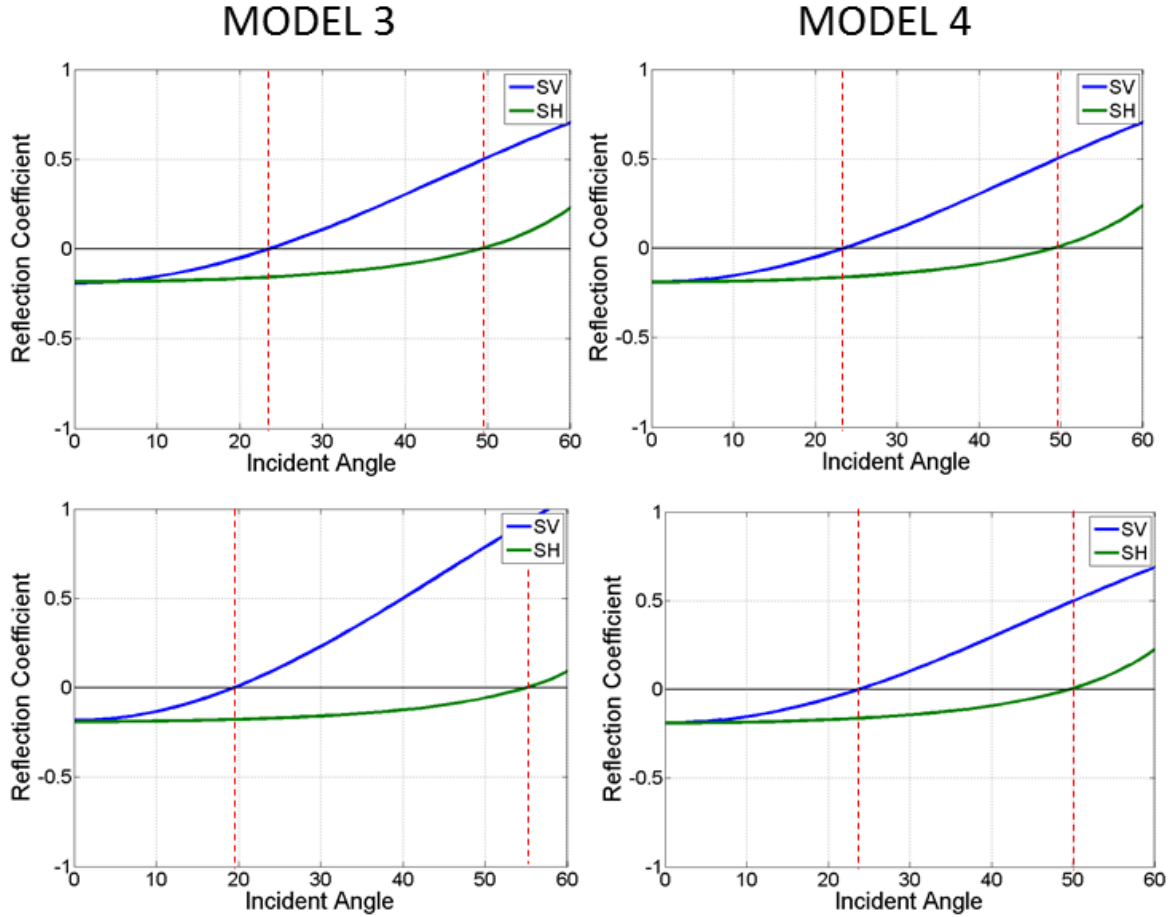


Figure 24. Shear-wave AVO. SH and SV reflection coefficients as a function of incidence angle. The interfaces are outlined above in table 3 and the graphs are calculated using Ruger’s equation for Isotropic over Transversely Isotropic medium. Note the red vertical lines show the zero crossings for the various models which are used to identify singularities in the polarization correction analysis. The top graph the source is oriented parallel to fractures and the lower plots the source is oriented perpendicular to fractures. Note there is no change in zero crossing.

In order for us to apply the polarization correction to 3D seismic data we need to rotate the field-coordinate data into radial-transverse coordinates which produces true separation of *SH* data from *SV* data in the context of an isotropic, flat-layered earth. This will be demonstrated on 3D–9C data set in a structurally complex area of interest for real data applications

CONCLUSIONS

The reflection process alters the polarization of a direct shear wave in isotropic media. The change in the individual *SV* and *SH* reflection coefficients with incidence angle (figure 1)

Corrections for Polarization Distortion

determines where and to what degree the polarization is altered. A correction which removes the distorting AVO effect results in a reflected polarization more in line with the input polarization. We might postulate a universal correction in order to be applied to any seismic data set in the future.

The correction was developed using synthetic seismic data sets within a 3D survey, and will be used on a 3D data set after rotation into *SV* and *SH* coordinates.

After applying the correction to the synthetic models we now have a viable correction to apply to account for the survey geometry effect on shear wave polarization (prior to polarization analysis for fracture characterization). Survey geometry is very important in understanding reflected shear polarization even in a purely isotropic media. Removing the AVO effect by applying a two term correction of amplitude variation with angle to the *SV* and *SH* components it works reasonably well and there is much work to be done in applying it to real seismic data.

ACKNOWLEDGMENTS

The EDGER Forum at the University of Texas at Austin partially supported this work.

REFERENCES

Alford, R. M., 1986, Shear data in the presence of azimuthal anisotropy: Dilley, Texas: 56th Ann. Internat. Mtg., Soc. Expl. Geophys., Expanded Abstracts, 476–479.

Corrections for Polarization Distortion

- Bowman, J. R., and M. A. Ando, 1987, Shear-wave splitting in the upper mantle wedge above the Tonga subduction zone: *Geophys. J.R. Astron. Soc.*, **88**, 25-41.
- Crampin, S., 1983a, Effects of anisotropy on reflectivity: 53rd Ann. Internat. Mtg, Session:RW2.8, Soc. of Expl. Geophys.— 1983b, Shear wave polarizations: A plea for three-component recording: 53rd Ann. Internat. Mtg, Session:S12.7, Soc. of Expl. Geophys.
- Gumble, J. E., 2006, Complete Anisotropic analysis of three component seismic data related to the marine environment and comparison to nine component land seismic data, Ph.D. Dissertation, University of Texas at Austin.
- Krohn, C. E., 1988, Computer modeling of P-SV waves: 58th Ann. Internat. Mtg, Session: S13.5, Soc. of Expl. Geophys.
- Lyons, E. S., 2006, Polarization rotation upon reflection of direct shear waves in purely isotropic media, MS Thesis, University of Texas at Austin.
- Mallick, S. and L. N. Frazer, 1987, Practical aspects of reflectivity modeling, *Geophysics*, **52**, 1355-1364
- Martin, M.A., and T.L. Davis, 1987, Shear-wave birefringence: A new tool for evaluating fractured reservoirs: *The Leading Edge*, Society of Exploration Geophysicists, October, 1987, p. 22-28.
- Ruger, A. 1996, P-wave reflection coefficients for transversely isotropic models with vertical and horizontal axis of symmetry
- Ruger, A., 1996, Reflection coefficients and azimuthal AVO analysis in anisotropic media, PhD Thesis, T-4946, Colorado School of Mines, 170 p
- Sheriff, R. E. and L. P. Geldart, 1995, *Exploration seismology*, 2nd ed.: Cambridge University Press.
- Simmons, J., and M. Backus, 2001, Shear waves from 3-D-9-C seismic reflection data: Have we been looking for signal in all the wrong places? *The Leading Edge*, **20**, 604–612,
- Simmons, J., 2004, Multicomponent Prestack Modeling in Isotropic/Anisotropic Media: Annual Meeting, CSEG, S083.
- Spratt, R. S., N. R. Goins, and T. J. Fitch, 1993, Pseudo-shear - The analysis of AvO, *in* Backus, M. M., ed., *Offset-dependent reflectivity - theory and practice of AVO analysis*, 37–56. Soc. of Expl. Geophys.
- Tatham, R. H. and M. D. McCormack, 1991, *Multicomponent Seismology in Petroleum Exploration*: SEG, Edited by E. B. Nietzel and D. F. Winterstein.
- Tatham, R. H., M. D. Matthews, K. K. Sekharan, C. J. Wade, and L. M. Liro, 1992, A physical model study of shear-wave splitting and fracture intensity: *Geophysics*, **57**, 647–652.
- Thomsen, L., 1986, Weak elastic anisotropy: *Geophysics*, V.51, No 10, p. 1954-1966.
- Thomsen, L., 2002, Understanding seismic anisotropy in exploration and exploitation, SEG